Algorithm Application to Improve Weather Radar Snowfall Estimates for Winter Hydrologic Modelling

S.R. FASSNACHT,[1] E.D. SOULIS[1] AND N. KOUWEN[1]

ABSTRACT

Algorithms were applied to weather radar data to improve the precipitation estimation for winter hydrologic modelling. The radar data were adjusted to consider the occurrence of mixed precipitation at above freezing air temperatures, the shape of snow particles, and a site specific scaling phenomena. Radar data, uncorrected and corrected gridded gauge precipitation data were used as input to the linked WATFLOOD/CLASS hydrologic model for simulation of streamflow. WATFLOOD performed the horizontal water routing and CLASS performed the vertical energy and water budgetting. Modelling of the Grand River watershed that is within the coverage of the Atmospheric Environment Service C-band radar in King City, Ontario, Canada for the five winters from 1993 to 1997 illustrated that on average the adjusted radar images produced ± 15% of the observed runoff volumes whereas the corrected gauge precipitation yielded 35% less runoff than observed. Substantial seasonal variation was observed. Radar provided more realistic winter precipitation quantities for streamflow modelling than the corrected gauge data. Application of the algorithms improved upon the raw radar estimates.

Key words: hydrologic modelling, weather radar, precipitation gauges, winter hydrology, snow

INTRODUCTION

In areas of the world that are covered with snow for a portion of the year, a significant volume of the yearly hydrograph can be contributed by snowmelt, which generates an interest in hydrologic modelling for forecasting of late winter streamflows. Hydrologic modelling for the purpose of predicting the spring snowmelt hydrograph often starts late in the season or at the onset of melt using estimates of the state of the snowpack that have been derived from snowcourse data or remotely sensed estimates of snowcovered area (eg. active microwave satellite imagery) and snow water equivalence (SWE) (eg. passive microwave).

A different approach is to model the duration of the winter using precipitation as input and estimates of the state of the snowpack for validation. The initialization of the continuous method can start at any time before the first snow accumulation, unlike the snowmelt modelling where the forecaster attempts to catch the start of melt. However, instead of only modelling snowmelt, all winter processes must be modelled and good estimates of snowfall are required.

Traditionally, the approximation of snowfall quantities has used point estimates of depth and SWE by precipitation gauges, yet there are a number of errors associated with this type of measurement. For the World Meteorological Organization Solid Precipitation Measurement Intercomparison, Goodison *et al.* (1998) summarized the various errors, derived correction methods, and established a reference method for intercomparison of any precipitation gauge type. Among the most significant problems

[1] Department of Civil Engineering, University of Waterloo, Waterloo, Ontario N2L 3G1, Canada

were the systematic errors caused by wind under-catch, wetting, and evaporation losses. To establish a reference method, the bush shield, the double fence shield, the forest clearing, the snow board, and the double gauge system were considered. Goodison *et al.* (1998) stated that while the natural bush shelter provided the best estimate of ground truth, such a setting was not available in all climatic regions (eg. high alpine and polar regions) and an artificial shield was recommended instead. The Tretyakov gauge with an octagonal vertical Double Fence was established as the Intercomparison Reference (DFIR) gauge.

To correct for the under-estimation due to wind, best fit regression equations were derived as a function of gauge height wind speed. For the Nipher-shielded gauge that is used as the Canadian standard snow measurement gauge, Goodison *et al.* (1998) derived the following relationship for the catch ratio of a Nipher-shielded gauge with respect to the DFIR gauge:

$$\frac{NIPHER}{DFIR}(\%)_{snow} = 100 - 0.44U_{gauge}^2 - 1.98U_{gauge} \quad (1),$$

where U_{gauge} is the wind speed (in m/s) at the gauge height.

Other underestimation errors may be due to bridging across the gauge mouth and sticking to the sides of the gauge, and hence the precipitation is not weighed (Cole *et al.* 1998). This has been partially overcome by the use of heated gauges that melt the frozen precipitation, but this may lead to evaporative losses. Goodison (1978) measured the wetting loss for the Nipher-shielded gauge to be 0.15mm +/- 0.02mm, and 0.2mm for the Tretyakov gauge used with the DFIR. Goodison and Metcalfe (1992) stated that Russia has used a wetting loss correction of 0.2mm for liquid precipitation and 0.1mm for solid precipitation, and they subsequently recommended that 0.15mm should be added to each observation to correct for wetting loss.

While gauge snowfall estimates can be corrected to consider most systematic errors in gauge snowfall estimation, the gridding of these point data produces questionable areal estimates, especially where gauge data are sparse. Numerous methods have been developed for the spatial interpolation of data. For the gridding of point precipitation data, Thiessen (1911) estimated the average areal precipitation for large areas. Since then, many of the interpolation schemes have focused on developing appropriate weighting functions for the distance weighting scheme (see Tabios and Salas 1985; and Bussieres and Hogg 1989 for a summary). The quality of the gridded data with respect to the actual precipitation that fell over the same area is often uncertain, as it is in part a function of the location, quantity, and quality of the point data. To this end, Marsh (1990) stated that for northern regions, "there is a drastic need to increase the density of the precipitation network through the installation of remote stations or weather radars."

Weather radar can provide the spatial distribution of precipitation with a temporal representivity of one hour or less. It has been used extensively to estimate rainfall rates by relating reflectivity of falling particles (Z) to precipitation rate (R). The Z-R relationship, initially developed by Marshall and Palmer (1948) for rainfall, is based on observations of individual storms and theoretical analysis related in part to drop size distributions. Numerous Z-R relationships have been developed for snowfall (Fujiyoshi *et al.* 1990 provides a good summary of previous Z-R relationship determinations). Most are based on individual storm events and involve comparisons to precipitation gauges. The analysis by Sekhon and Srivastava (1970) developed the Z-R relationship that is widely used for the cold weather season precipitation estimation. Recently the advanced capabilities of weather radar have been explored to examine complex snowfall. For example, Ryzhkov and Zrnic (1998) used polarimetric radar to distinguish between rain and snow, and Matrosov (1998) showed that the difference between the reflectivities at the dual wavelengths yielded a snowflake size estimate that could be combined with the longer wavelength reflectivity to approximate a snowfall rate.

While weather radar has been used to estimate rainfall across watersheds for modelling purposes in numerous studies, including Kouwen and Garland (1989) and Finnerty *et al.* (1997), its application

to winter modelling has been very limited. To date, Houck *et al.* (1995) has recommended the use of weather radar snowfall estimates as input to a GIS hydrological analysis, and Fassnacht *et al.* (1998a) employed weather radar for the modelling of 1993 winter season on the Grand River basin in southern Ontario.

This research examined the effectiveness of weather radar to estimate precipitation for hydrologic modelling of the entire winter, and specifically focused on the comparison of the following precipitation datasets: uncorrected and corrected gridded gauge precipitation and various forms of raw and adjusted weather radar precipitation. In particular, the radar data were adjusted to consider the occurrence of mixed precipitation at above freezing air temperatures and the implication of the shape of snow particles at below freezing air temperatures. For rain in winter, a constant adjustment factor and a variable adjustment factor that are functions of the precipitation rate were considered. A scaling phenomena associated with the radar data is also discussed. The success of each algorithm was assessed in terms of the peak flows and runoff volumes in the Grand River watershed in southern Ontario for the five winters from 1993 to 1997 (each spanning the months of November to April).

STUDY AREA

The winter hydrology was modelling for the Upper Grand River watershed, located in central south-western Ontario (see Fig. 1). Most of this watershed is covered by crops and low vegetation (59%), with smaller regions of wetland (18%) and mixed deciduous-coniferous forest (14%). The remainder of the watershed comprises bare (8%) and impervious (1%) areas. The terrain in this portion of southern Ontario is glacial material, composed primarily of clayey till. There are eight hydrometric stations within the study basin where streamflow is monitored (see Table 1 and Fig. 2).

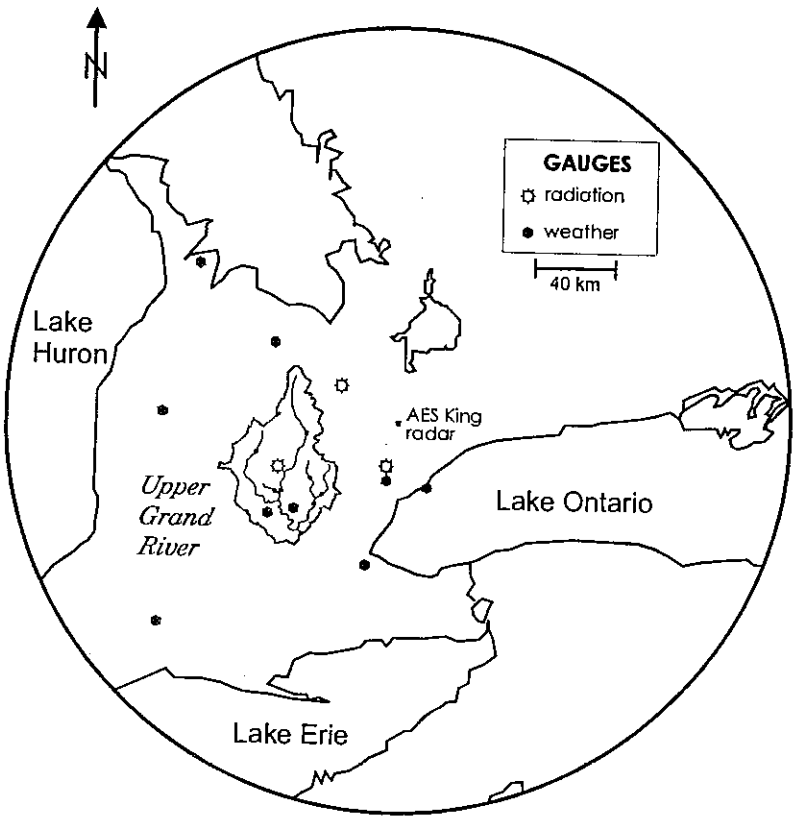

Figure 1. Location map of the Upper Grand River watershed within central southern Ontario.

Table 1. Description of the eight hydrometric stations within the Grand River basin that are used in this analysis.

hydro-metric station	gauge number	location	drainage area (km^2)	latitude (N)	longitude (W)
1	02GA003	Grand River at Galt	3520	43°21'10"	80°19'01"
2	02GA034	Grand River near West Montrose	1170	43°35'06"	80°28'54"
3	02GA014	Grand River at Marsville	694	43°51'43"	80°16'22"
4	02GA029	Eramosa River above Guelph	236	43°32'52"	80°10'59"
5	02GA039	Conestogo River above Drayton	272	43°46'58"	80°38'20"
6	02GA040	Speed River at Armstrong Mills	167	43°38'19"	80°16'12"
7	02GA015	Speed River below Guelph	593	43°31'30"	80°15'44"
8	02GA023	Canagagique Creek near Elmira	118	43°34'46"	80°30'30"

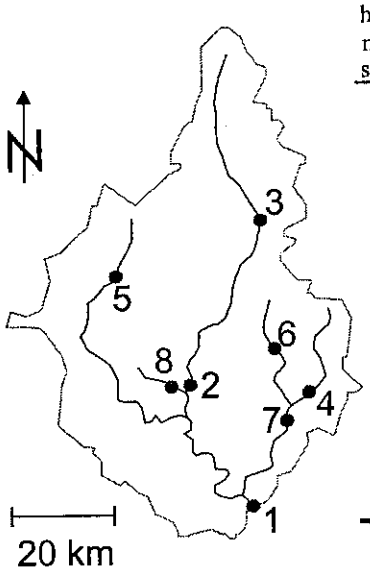

Figure 2. Location of the eight hydrometric stations within the Upper Grand River basin.

The Grand River basin is located within the coverage of the Atmospheric Environment Service King City Radar, which is located at (43 ° 57' 50"N, 79° 34' 27"W). The installation is primarily a C-band radar (5.2 cm), although it has X-band capabilities. It provides a conventional radar image with a 2 x 2 km grid over a scanning radius of 200 km. The hourly precipitation accumulation maps are rates in millimetres of water. These radar maps are prepared from 10 minute Constant Altitude Plan Position Indicator images, based on the radial hit closest to centre of the square grid pixel. For the warm season, the power law reflectivity-precipitation rate relationship developed for southern Ontario by Richards and Crozier (1983) is used, and for the cold season, the Sekhon and Srivastava (1970) relationship is used (Crozier *et al.* 1991). The radar data are averaged from the entire scenes of 2 by 2 km pixels for the 10 by 10 km grid elements using software written in part by the image providers (Mould 1985).

METHODOLOGY

The usefulness of radar to estimate snowfall as precipitation input for hydrologic modelling of a watershed was examined as a comparison of streamflows simulated from gridded gauge precipitation and radar estimates. The improvements of these estimates by the application of several algorithms are also presented in this paper.

Hydrologic modelling

The hydrology of the watershed was simulated using the distributed hydrologic model WATFLOOD, developed at the University of Waterloo (Tao and Kouwen 1989), that has been linked with the land surface scheme CLASS, developed by Environment Canada (Verseghy 1991). Details of the linkage are presented in Soulis *et al.* (1999). The vertical water and energy budgets near the land surface are computed using CLASS, while the lateral water budget and streamflow routing is performed using WATFLOOD. Snow is accumulated into a single layer pack and budgeting is

performed using heat and moisture transfer considerations. The following snow processes are considered in CLASS: surface albedo, snowpack density, effective thermal conductivity, snow heat capacity, short-wave radiation density fluxes, sublimation, snowmelt, and meltwater evaporation. Both models use the mosaic or Grouped Response Unit approach (Kouwen *et al.* 1993) to incorporate land cover heterogeneity within grid elements. The grid elements are normally square and usually range from 2 to 50 kilometres in length. Up to 15 different land covers types can exist within each grid element, each of which has different soil and vegetation properties. The Upper Grand River basin was modelled using 10 by 10 km grid elements, for which the slope and flow direction have previously been determined (Tao and Kouwen 1989). Aspect was not considered at this scale.

Gauge Precipitation Correction

According to Environment Canada (1998), hourly rainfall rates are measured using a tipping bucket gauge whereas snowfall rates are measured using a Nipher-shielded gauge. Therefore, it was assumed that once precipitation occurred at temperatures below freezing (November 1st or later) the precipitation rates were measured using a Nipher-shielded gauge and the appropriate wind under-catch and wetting loss corrections could be applied. It was also assumed that once the daily minimum temperatures no longer go below freezing (April 30 th at the latest), precipitation data were collected using a tipping bucket gauge.

While a DFIR gauge provides good estimates of snowfall, it must be adjusted to approximate the "true" snowfall, as measured in a sheltered bush. The Nipher-shielded gauge data was corrected to the DFIR gauge data and these data were subsequently corrected to the bush gauge data. Equation (1) was inverted to yield a ratio:

$$\frac{DFIR}{NIPHER} = \frac{100}{100 - 1.98U_{gauge} - 0.44U_{gauge}^2} \qquad (2).$$

Yang *et al.* (1993) derived six different ratios between the bush gauge and DFIR for different types of precipitation. Plotting of these six relationships on the same axes (Figure 3) illustrates that the differentiation of precipitation is only significant for blowing snow. As a second order polynomial, the average bush to DFIR gauge ratio takes the form:

$$\frac{BUSH}{DFIR}(\%)_{avg} = 99.04 + 1.639U_{gauge} + 0.0857U_{gauge}^2 \qquad (3).$$

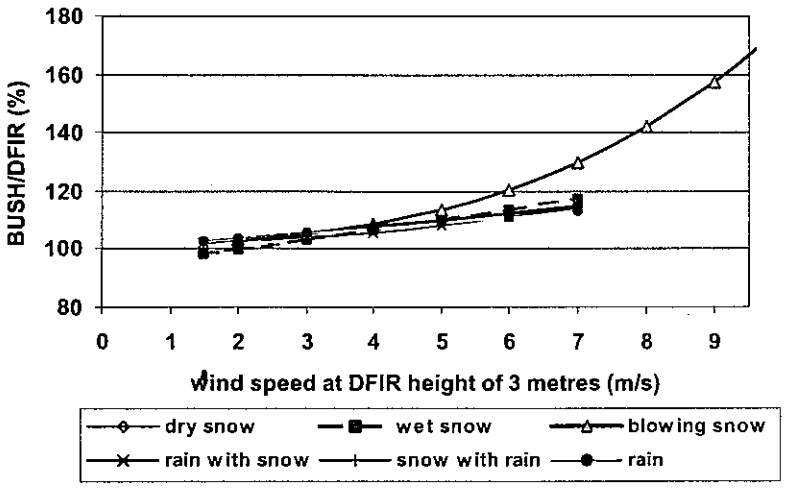

Figure 3. Ratio of bush gauge to DFIR gauge as a function of wind speed for different precipitation types, using equations from Yang *et al.* (1993).

Prior to substitution of equation (2) into equation (3) to yield a relationship for the catch ratio of the bush gauge to the Nipher-shielded gauge, the wind speed at gauge height had to be compatible. Since a logarithm wind velocity distribution was assumed above the ground surface, for wind speeds measured at different heights, the wind speed (U_a) at one height (h_a) could be defined as a function the wind speed (U_b) at another height (h_b) as follows:

$$U_a = U_b \left[\frac{\log (h_a / z_0)}{\log (h_b / z_0)} \right] \quad (4),$$

where z_0 is the roughness length. Goodison *et al.* (1998) defined z_0 as 0.01m for the winter and 0.03m for the summer. Equation (2) assumes a wind speed (U_{NIPHER}) measured at a gauge height of 2m for the Nipher-shielded gauge, whereas equation (3) assumes a wind speed (U_{DFIR}) measured at a gauge height of 3m for Tretyakov in the DFIR. Using equation (4) for winter conditions, the wind speed at 2m was 92.89% of the wind speed at a 3m height or:

$$U_{DFIR} = 1.0765\ U_{NIPHER} \quad (5).$$

Equation (5) was substituted into equation (3) to yield:

$$\frac{BUSH}{DFIR}\ (\%) = 99.04 + 1.764 U_{NIPHER} + 0.0993 U_{NIPHER}^2 \quad (6).$$

Equation (6) was combined with equation (2) and, using regression analysis, was simplified to the catch ratio between bush and Nipher-shielded gauge:

$$\frac{BUSH}{NIPHER}\ (\%) = 106.2 - 2.228 U_{NIPHER} + 1.807 U_{NIPHER}^2 \quad (7),$$

which was used to correct the Nipher-shielded gauge data.

For the winter, precipitation may occur at above freezing temperatures, i.e., it can rain in the winter. Since the winter precipitation data are collected using a Nipher-shielded gauge, the gauge correction was applied for air temperatures less than 2.2°C. This temperature is the 50% percent probability of snow from the Auer (1974) relationship, and was the snow-rain threshold used by the BATS soil-vegetation-atmospheric-transfer model (Yang *et al.* 1998). To correct the Nipher-shielded gauge data for wetting loss, 0.15mm was added to each precipitation event.

Meteorological Data Gridding

The WATFLOOD/CLASS model requires the following meteorological data: air temperature, precipitation (as rain and snow), barometric pressure, specific humidity, wind speed and direction (defined in terms of north wind and east wind), and incoming shortwave and longwave radiation (see Table 2). All of the required meteorological data were measured at various locations across central south-western Ontario (see Fig. 1) and archived on an hourly basis, with the exception of specific humidity and longwave radiation. The specific humidity was derived from air temperature and relative humidity and the longwave radiation was computed from the air temperature and an estimate of the cloud cover.

Table 2. Summary of meteorological input data.

data field	description	units
temperature	air temperature	K
precipitation: rain	mass of liquid precipitation	m/s
precipitation: snow	mass of solid precipitation	m/s
barometric pressure	air pressure	mb
specific humidity	specific humidity	kg/kg
wind speed from north	north component of wind speed measured at 10m height	m/s
wind speed from east	east component of wind speed measured at 10m height	m/s
shortwave radiation	user defined, but often given as incoming	W/m^2
longwave radiation	user defined, but often given as incoming	W/m^2

There is a dense network of daily climate data available over southern Ontario, but few stations adequately measure hourly solid precipitation. Many of the stations only use the tipping bucket gauge (Environment Canada 1998). Goodison *et al.* (1998) stated that a tipping bucket gauges only catches one-third to one-half of the actual precipitation and that in Canada the tipping bucket gauge is only used for measuring liquid precipitation. No correction has been formulated to estimate the solid precipitation under-catch of a tipping bucket gauges. Therefore the tipping bucket gauge data were not used to generate the gridded precipitation fields. As well, only data from the synoptic stations and the three gauges operated by the University of Waterloo (see Fig. 1) were available for this work.

For central south-western Ontario, Tao and Kouwen (1989) used an inverse squared distance interpolation to grid rainfall and temperature data for grid block size of 10 by 10 km. This method and grid size were used in this research across the same study area.

When there is precipitation recorded at any one gauge, the distance weighting computes a precipitation quantity across the entire gridding domain. As this is an error associated with the interpolation scheme, gridded precipitation less than 0.01mm was assumed to be no precipitation and assigned a value of zero. For SWE measurements in Canada, a trace observation of snow is recorded 0.07 mm and 0.03 mm in the Arctic (Goodison *et al.* 1998).

Radar Data Adjustment

Radar precipitation estimates can cover areas up to 100,000 km^2 and provide a good representation of local intensity variations that are often not captured by the network of precipitation gauges that exist within the area. Snowfall precipitation rates measured by radar can be over or under-estimated by 100% or more (Fassnacht *et al.* 1998a). Some of the errors that can cause these discrepancies are forced over-scaling, mixed precipitation under-estimation, and signal variation due to different snow particle shapes. A comparison of corrected gauge versus radar accumulation for various adjustments to overcome these errors was provided in Fassnacht *et al.* (1998a). The following section provides a brief summary of the techniques used to adjust the radar data.

Scaling Removal

A simple problem that may cause overestimation of snowfall, especially for conventional radar, is forced over-scaling. This is a function of the discretization of the precipitation rates. For the King City Radar used in this research, there are 27 intervals at a minimum of 0.5 mm/h per increment. Forced over-scaling occurs when anomalous propagation is present that produces a return signal that is larger than the maximum rate (13.5 mm/h) at the lowest rate increment (0.5 mm/h). This forces an increase

in the scaling intervals to 1 mm/h, 2 mm/h or greater. This scaling increase may be appropriate for summer precipitation events, however, winter storms rarely produce hourly accumulation rates greater than 13.5 mm/h. To overcome the forced over-scaling, the radar data was reprocessed using only the lowest increment of 0.5 mm/h.

Previous research (Fassnacht *et al.* 1998a) illustrated that the removal of scaling for winter precipitation has improved the estimation of snowfall accumulation by radar in comparison to corrected gauge accumulation. The adjustment of the non-scaled images for the occurrence of mixed precipitation has further improved the monthly and seasonal accumulation estimates (Fassnacht *et al.* 1998a).

Mixed Precipitation

At temperatures near or slightly above freezing snowfall can melt, or be partially covered in water. The radar reflectivity from these melted or partially melted hydrometeors could be less than for some solid flakes, yet the precipitation intensity could be the same. Thus, application of the solid precipitation *Z-R* relationship at near or above freezing surface air temperatures may result in precipitation under-estimation.

Several relationships between probability of snow versus surface air temperature exist in the literature (USACE 1956 and Rohrer 1989), however these are all site specific. The snow versus air temperature probability curve derived by Auer (1974) was an average of 1000 stations across the mid-west US. As no relationship has been developed for central southern Ontario, the Auer curve was used to adjust the radar images for underestimation due to mixed and liquid precipitation. For air temperatures between +0.45 and +5.97 degrees Celsius, the following polynomial relationship was used to approximate the percentage of precipitation falling as snow, as a function of air temperature (T):

$$F_S = 0.0202T^6 - 0.3660T^5 + 2.0399T^4 - 1.5089T^3 - 15.038T^2 + 4.6664T + 100 \qquad (8).$$

Below a temperature of +0.45 °C it was assumed that there is 100% snow, and above +5.97 °C it is assumed that there is 100% rain. The percent snow (F_S) was used to adjust existing radar estimate (R_{old}) to produce a new radar estimate (R_{mixed}):

$$R_{mixed} = R_{old} \times F_S / 100 + (100 - F_S) / 100 \times \alpha R_{old}^{\beta} \qquad (9),$$

where α is the rain adjustment factor and β is the rain adjustment exponent. Assuming the same reflectivity and precipitation rate for a solid and liquid hydrometeor, the summer *Z-R* coefficients are 4.06 times larger than the winter coefficients. For hydrologic modelling using WATFLOOD, the authors have found that the summer radar coefficients often yield twice as much precipitation in terms of storm event hydrographs. Therefore, for the above 'mixed precipitation with constant R', α is 2.03 and β is 1.0.

The use of a 'constant R' was a good simplification for radar snowfall accumulation as it only used temperature for the image adjustment. To incorporate the radar precipitation rate into the adjustment, called 'variable R' for mixed precipitation, the manipulation of the summer and winter Z-R relationships yield a value of 2.165 for α and 1.545 for β.

Particle Shape

The shape of a snowflake will influence the reflectivity of a radar beam, and hence with the application of a single *Z-R* relationship, the snowfall rate. Ohtake and Hemni (1970) determined different *Z-R* relationships for different snowflake geometries. However, application of their

coefficients requires knowledge of the type of flake falling, which to date must be observed manually. A relationship has been developed from the growth rates of snow crystals to consider the surface area to mass ratio (SSA) of falling snowflakes. Various measurements of the rate of growth in a particle direction (axis) of a newly formed snow crystal as a function of temperature have been taken, and are summarized Ono (1970). To generate the SSA function, Ono's values were manipulated and normalized to yield a shape factor function with an approximate area equal to one. This function considers various snowflake shapes that form at different temperatures.

With the assumption that SSA is inversely related to snowfall rate (in terms of mass), the shape factor function can be inverted to yield the particle shape adjustment factor (F_{PS}) that, for air temperatures less than -1.0 degrees Celsius, can be expressed by the following third-order Fourier series:

$$F_{PS} = -1.75 \times [1.022 - 0.018 \times \cos(0.333\,T + 0.341) + 0.006 \times \cos(2 \times 0.333\,T + 0.341) - 0.029 \times \cos(3 \times 0.333\,T + 0.341) + 0.107 \times \sin(0.333\,T + 0.341) + 0.015 \times \sin(2 \times 0.333\,T + 0.341) - 0.017 \times \sin(3 \times 0.333\,T + 0.341) - 1] + 1 \quad (10).$$

Lautensach and Bogel (1956) stated that winter lapse rates in mid-latitude regions are close to zero. Therefore, the lapse rate between the snowfall formation height and the near surface where the air temperature is measured was assumed to be close to zero, and equation (10) was applied without further adjustment.

Table 3. Summary of precipitation input data.

source	specific form	short name	uncorrected	corrected
gauge	uncorrected nipher-shielded Belfort gauge	uncorrected gauge	X	
	gauge data corrected to DFIR gauge	gauge corrected to DFIR		X
	gauge data corrected to "bush" gauge	gauge corrected to "bush"		X
radar	raw C-band weather radar images	raw	X	
	radar with variable scaling removed	no scaling		X
	no scaling radar with mixed precipitation consideration ($\alpha = 2.03$, $\beta = 1.0$)	mixed precip.		X
	no scaling radar with mixed precipitation ($\alpha = 2.03$, $\beta = 1.0$) and particle shape considerations	mixed/particle shape		X
	no scaling radar with mixed precipitation consideration ($\alpha = 2.165$, $\beta = 1.545$)	mixed with variable R		X
	no scaling radar with mixed precipitation ($\alpha = 2.165$, $\beta = 1.545$) and particle shape considerations	mixed/part with variable R		X

Adjustment Procedure

The gauge and radar data with the various corrections and adjustments that are used as precipitation input are summarized in Table 3. The 'raw' radar data are those images derived without any adjustment. The 'no scaling' data are obtained by resetting the scale in each image to the minimum value. These 'no scaling' data are then used to derive the various temperature adjusted images. In the

'mixed precipitation' image rates are adjusted for temperatures above +0.45 °C, whereas the 'mixed precipitation / particle shape' image uses adjustment for mixed precipitation and the particle shape function, i.e., for all observed temperatures. For the temperature adjustments, both a constant precipitation rate and a variable precipitation rate are applied to consider mixed precipitation. The particle shape adjustment is not considered a function of the precipitation rate.

RESULTS AND DISCUSSION

The observed streamflows at the eight stations within the Upper Grand River basin can be compared to the simulated hydrograph derived from gauge and radar precipitation inputs. The observed streamflows were measured by the Grand River Conservation Authority and Water Survey of Canada and are available from HYDAT (Environment Canada 1997). A sample hydrograph comparison for December 1993 to April 1994 on the Grand River at Galt (gauge 02GA003) is presented in Fig. 4a through 4e. The increased flows at the end of January and mid-February are not simulated well from any of the precipitation modelling inputs (uncorrected gauge, DFIR gauge, "bush" gauge, raw radar or radar adjusted for mixed precipitation and particle shape). Correction of gauge precipitation for wind under-catch improved the estimation of the first peak snowmelt flow in late March, but the subsequent peaks are all still underestimated. For this location and year, the volume of spring meltwater is better estimated using the radar precipitation than the corrected gauge precipitation. Use of the adjusted radar precipitation improved the modelling of the initial snowmelt peak (Fig. 4e) as compared to the streamflow overestimation by the raw radar (Fig. 4d).

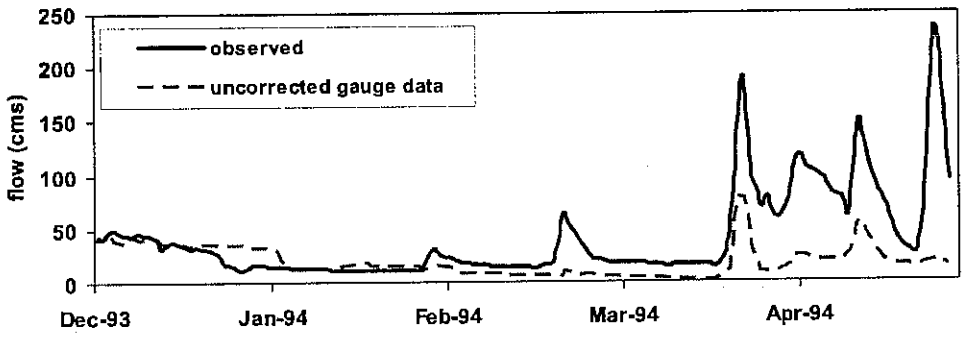

Figure 4a. December 1993 to April 1994 observed (solid) and simulated (dashed) streamflow at the Grand River at Galt derived from (a) uncorrected gauge data.

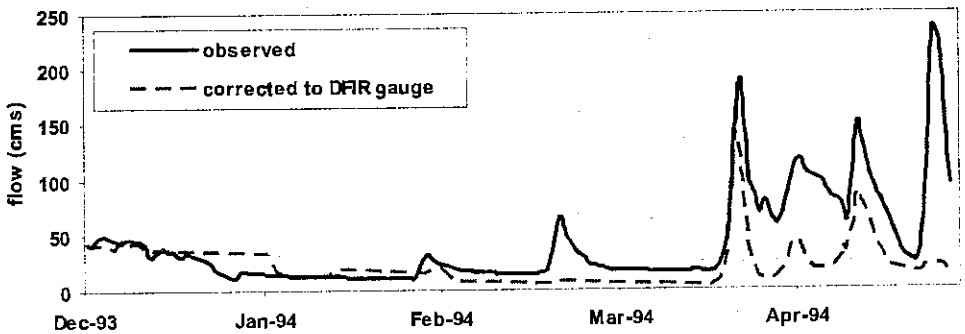

Figure 4b. December 1993 to April 1994 observed (solid) and simulated (dashed) streamflow at the Grand River at Galt derived from (b) gauge data corrected to DFIR gauge.

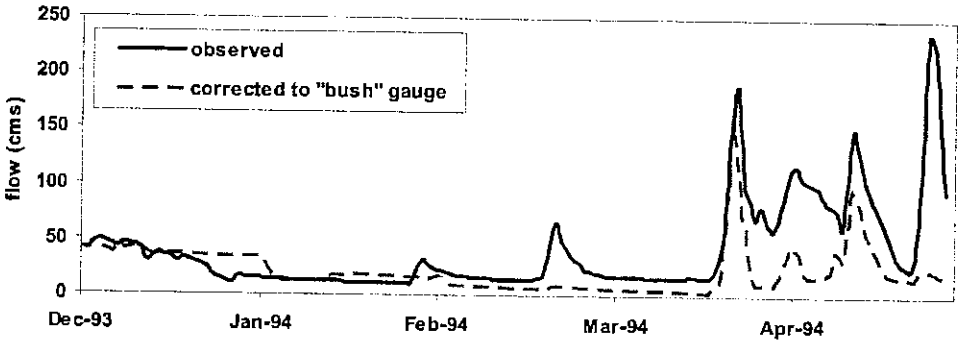

Figure 4c. December 1993 to April 1994 observed (solid) and simulated (dashed) streamflow at the Grand River at Galt derived from (c) gauge data corrected to "bush" gauge.

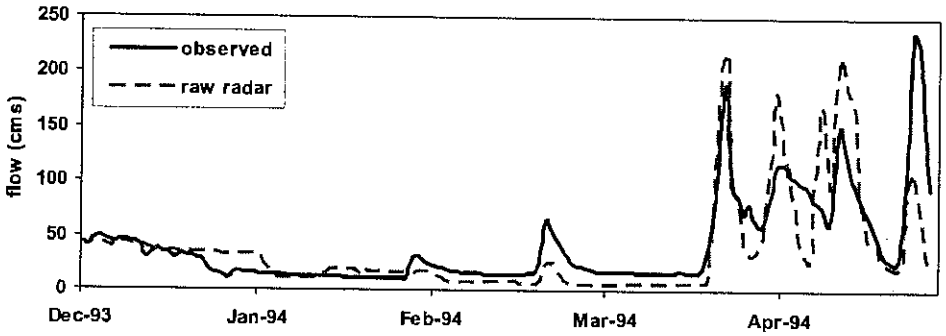

Figure 4d. December 1993 to April 1994 observed (solid) and simulated (dashed) streamflow at the Grand River at Galt derived from (d) raw radar

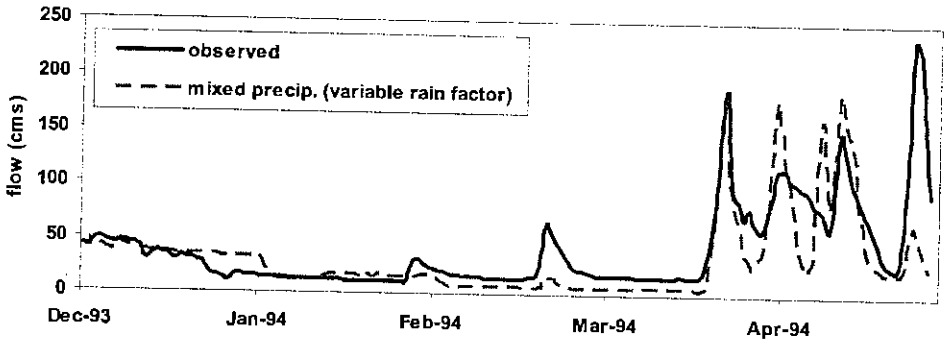

Figure 4e. December 1993 to April 1994 observed (solid) and simulated (dashed) streamflow at the Grand River at Galt derived from (e) radar adjusted for mixed precipitation (variable rain factor) and particle shape.

The observed annual peak flows at each gauge for the five winter season (1993-1997) is compared to the modelled peak flows for the nine different modelling inputs (summarized in Table 3) in Figures 5a through 5i. The uncorrected and corrected (DFIR and "bush") gauge precipitation inputs underestimate the peak flow for most winters at most gauges (Fig. 5a, b, and c respectively), while there are similar results from all the different radar datasets. The largest overestimate of streamflow results from using the raw radar input. Slightly improved flows result from use of the radar adjusted for mixed precipitation using the variable R (Fig. 5h) and from the radar subsequently adjusted for particle shape (Fig. 5i).

Statistics that accompany the computed versus observed peak flows are presented in Table 4. For the best fit line through the origin, the best correlation occurred for the uncorrected gauge precipitation, followed by the two corrected gauge precipitation scenarios. However, these correlations correspond to slopes that are 34.6, 22 and 23.2% less than the optimal slope of unity. The best fit

Table 4. Summary of peak flow statistics for all the five winters of peak flow data. The nine precipitation input data are as summarized in Table 3.

	precipitation gauge data			radar data					
statistic	uncorrected gauge	gauge corrected to DFIR	gauge corrected to "bush"	raw	no scaling	mixed precip	mixed / particle shape	mixed with variable R	mixed/ part with variable R
slope (y-int. = 0)	0.654	0.780	0.768	1.006	0.956	1.092	1.105	0.835	0.853
r^2	0.806	0.717	0.714	0.575	0.596	0.645	0.650	0.540	0.556
r^2 (slope = 1, y-int. = 0)	0.452	0.639	0.620	0.600	0.619	0.661	0.663	0.518	0.545
average difference (m^3/s)	-38.1	-22.3	-23.1	7.9	2.7	14.1	16.1	-7.6	-5.6

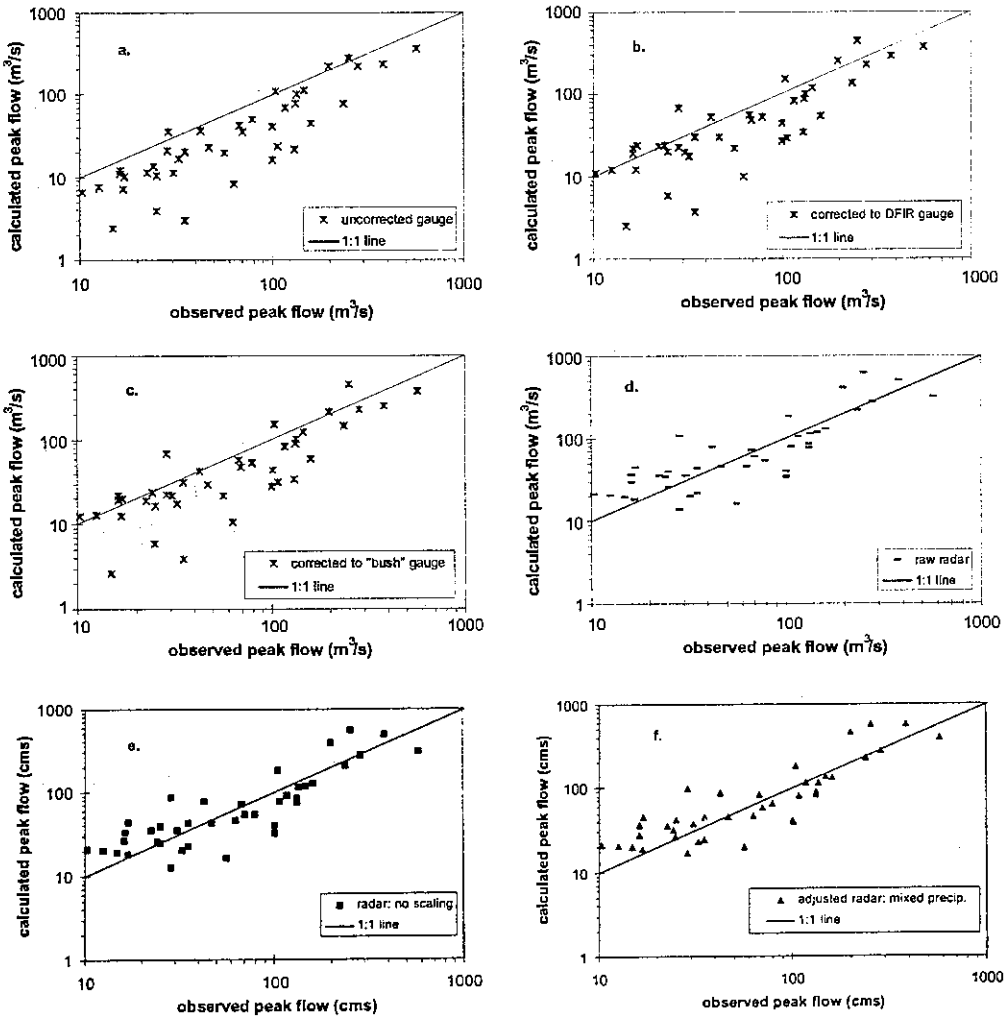

Figure 5. Observed versus calculated peak flow for the 1993 to 1997 winters using (a) uncorrected gauge data, (b) gauge data corrected to DFIR gauge, (c) gauge data corrected to "bush" gauge, and (d) raw radar input.

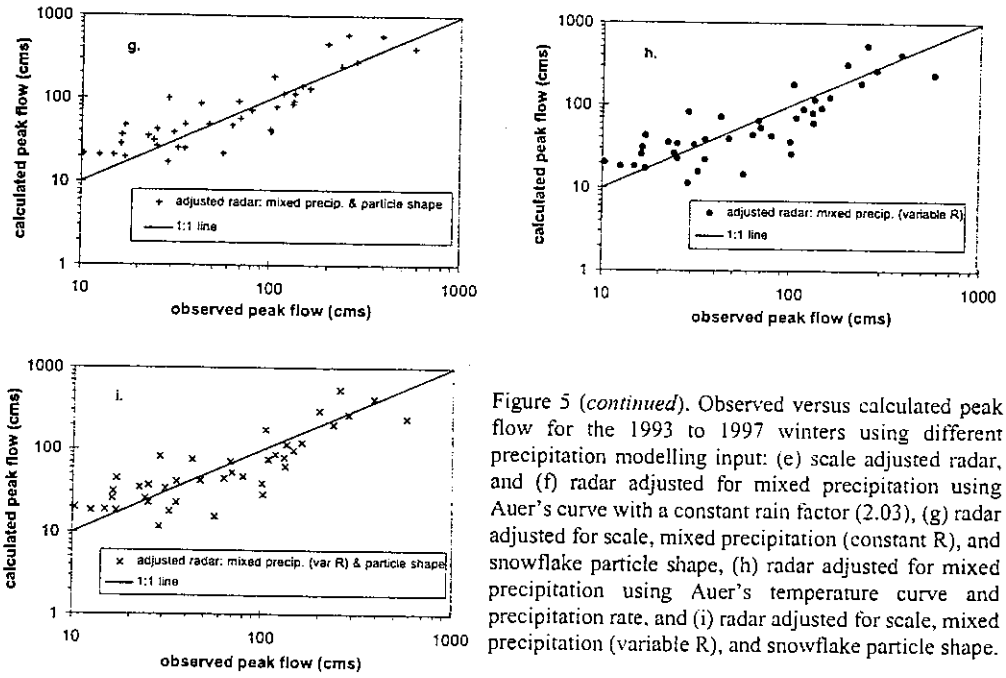

Figure 5 (*continued*). Observed versus calculated peak flow for the 1993 to 1997 winters using different precipitation modelling input: (e) scale adjusted radar, and (f) radar adjusted for mixed precipitation using Auer's curve with a constant rain factor (2.03), (g) radar adjusted for scale, mixed precipitation (constant R), and snowflake particle shape, (h) radar adjusted for mixed precipitation using Auer's temperature curve and precipitation rate, and (i) radar adjusted for scale, mixed precipitation (variable R), and snowflake particle shape.

slopes for all the radar datasets are closer to unity. Using a best fit line through the origin with a slope of unity, the correlation for the peak flows generated from the two corrected gauge precipitation scenarios is only slightly less than the mixed precipitation and mixed precipitation with particle morphology considerations (constant R). The peak flows from the two corrected gauge precipitation simulations are clustered below the 1:1 line, while the peaks from the two 'constant R' simulations are above the 1:1 line. On average, modelling using the no scaling radar scenario yields the peak flows closest to the observed. The computed peak flows are an integration of the WATFLOOD/CLASS model, however, the total seasonal runoff volumes are a better indication of the adequacy of precipitation dataset. Unpublished studies have shown that WATFLOOD (Seglenieks *et al.* 1997) and WATFLOOD/CLASS (Fassnacht *et al.* 1998b) convert almost all precipitation data into runoff over a year. For a simulation of the period from January to June 1993 using raw radar as the precipitation input, the water budget of approximately 400mm precipitation closed to within 10% (Fassnacht *et al.* 1998b).

The two sample cumulative runoff volumes presented in Figures 6a and 6b for the 1993 winter on the Eramosa River above Guelph and for the 1996 winter on the Speed River at Armstrong Mills, illustrate that the different radar datasets yield similar total runoff volumes that are double the flow volumes modelled using the gauge precipitation input. In 1993, the main difference between the three radar datasets resulted from a rain on ice event that occurred in early January. Similarly, a mid-January 1996 melt event caused the primary difference in the runoff volumes modelled with the radar data.

The winter season runoff volumes for eight stations using the three gauge precipitation and six radar products are summarized in Table 5a through 5e for the five winters. For all years and at all streamflow stations, hydrologic modelling with the uncorrected gauge precipitation underestimates flow in comparison to observed flow. The same holds true for the corrected gauge precipitation data, with the exception of the winter of 1995 where the DFIR and "bush" gauge precipitation yielded 8 to 10% more water than observed (Table 6).

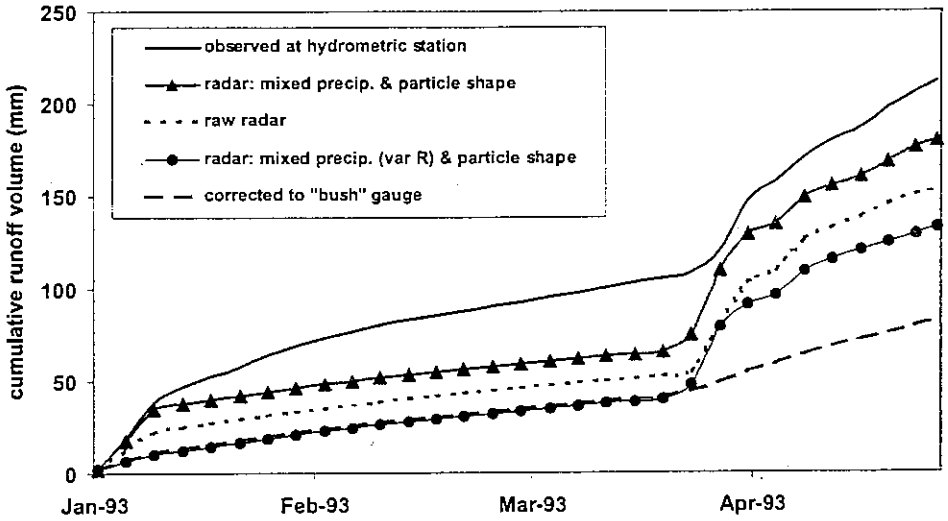

Figure 6a. Cumulative runoff volume from Jan. 1993 to April 1993 on the Eramosa River above Guelph.

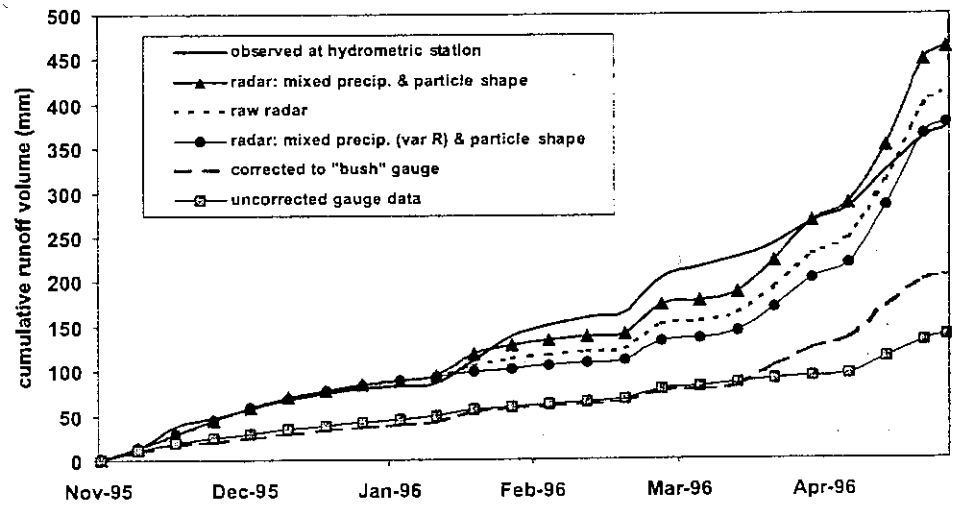

Figure 6b. Cumulative runoff volume from Nov. 1995 to April 1996 on the Speed River at Armstrong Mills.

Table 5a. January 1993 to April 1993 winter runoff volumes (mm) at eight streamflow gauges (column 1) for the observed (column 2) and simulated runoff volumes based on the precipitation inputs summarized in Table 3.

		simulated runoff volume from different precipitation inputs (mm)								
		precipitation gauge data			radar data					
stream flow gauge [1]	observed runoff (mm) [2]	uncorrected gauge	gauge corrected to DFIR	gauge corrected to "bush"	raw	no scaling	mixed precip	mixed / particle shape	mixed with variable R	mixed/part with variable R
1	205	127	129	130	171	169	182	185	157	160
2	207	136	136	137	156	156	161	163	151	152
3	241	92	98.1	99.2	152	150	174	177	133	135
4	212	77.1	81.3	82.2	154	148	174	180	129	133
5	235	113	119	120	211	209	243	248	183	187
6	231	81.4	85.5	86.7	164	160	187	193	139	144
7	192	139	141	142	191	187	204	208	174	177
8	188	87.3	90.7	91.7	175	172	196	203	150	156

Table 5b. December 1993 to April 1994 winter runoff volumes, as in Table 5a.

		simulated runoff volume from different precipitation inputs (mm)								
		precipitation gauge data			radar data					
stream flow gauge	observed runoff (mm)	uncorrected gauge	gauge corrected to DFIR	gauge corrected to "bush"	raw	no scaling	mixed precip	mixed / particle shape	mixed with var. R	mixed/part with variable R
1	153	72.1	81.9	84.1	136	134	144	146	123	125
2	145	51.6	56.2	57.3	82.9	81.5	86	86.7	76.2	76.6
3	157	102	115	117	199	193	212	214	175	178
4	149	87.7	103	106	194	190	210	211	169	170
5	180	137	158	162	299	292	316	319	267	271
6	170	98.9	117	120	220	215	237	238	190	191
7	123	79	89.3	91.7	148	145	158	159	131	132
8	187	112	131	135	260	255	275	279	229	241

Table 5c. November 1994 to April 1995 winter runoff volumes, as in Table 5a.

		simulated runoff volume from different precipitation inputs (mm)								
		precipitation gauge data			radar data					
stream flow gauge	observed runoff (mm)	uncorrected gauge	gauge corrected to DFIR	gauge corrected to "bush"	raw	no scaling	mixed precip	mixed / particle shape	mixed with var. R	mixed/part with variable R
1	182	156	200	205	360	294	344	350	247	254
2	182	158	197	201	341	281	325	331	241	248
3	205	154	188	191	345	283	326	333	245	253
4	164	140	175	178	408	321	401	406	254	259
5	267	207	264	269	479	391	451	459	342	351
6	207	157	200	205	339	281	337	342	232	238
7	149	148	189	193	372	301	367	372	242	249
8	179	172	222	228	352	287	333	337	243	249

Table 5d. November 1995 to April 1996 winter runoff volumes, as in Table 5a.

		simulated runoff volume from different precipitation inputs (mm)								
		precipitation gauge data			radar data					
stream flow gauge	observed runoff (mm)	uncorrected gauge	gauge corrected to DFIR	gauge corrected to "bush"	raw	no scaling	mixed precip	mixed / particle shape	mixed with var. R	mixed/part with variable R
1	307	119	155	164	323	320	354	358	292	296
2	331	108	126	139	268	266	296	298	241	244
3	385	155	171	205	382	381	403	406	363	365
4	285	120	160	173	376	375	412	416	352	358
5	465	195	240	273	574	570	603	609	530	539
6	373	138	184	206	413	410	455	463	370	379
7	245	114	148	159	326	325	364	367	297	302
8	282	158	214	237	456	453	488	497	420	426

The various radar adjustment schemes provide improved flow estimates, yet significant seasonal variation exists. For 1993, the computed runoff volumes are 8 to 28% less than the observed flows, partly due to underestimation of the early January storm event. The 1994 and 1996 runoff volumes are overestimated by an average of 18 and 19%, with a range of 7 to 40% and 1 to 50% respectively. The Grand River streamflow stations at Galt and near West Montrose were underestimated for 1994 and 1996. There was, on average, a 70% overestimation of runoff volumes in 1995. The computed 1997 streamflows were less than half of the observed flows. Fassnacht *et al.* (1998a) and Hollingsworth (pers. comm., 1999) also saw significant radar snowfall underestimation in 1997.

Table 5e. December 1996 to April 1997 winter runoff volumes, as in Table 5a.

		simulated runoff volume from different precipitation inputs (mm)								
		precipitation gauge data			radar data					
stream flow gauge	observed runoff (mm)	uncorrected gauge	gauge corrected to DFIR	gauge corrected to "bush"	raw	no scaling	mixed precip	mixed / particle shape	mixed with var. R	mixed/part with variable R
1	328	171	192	195	167	166	196	201	142	146
2	354	167	185	188	159	158	184	188	136	140
3	381	158	173	177	148	147	171	175	128	131
4	332	133	152	155	146	145	170	175	125	130
5	521	229	253	257	218	216	253	259	185	191
6	465	162	185	188	165	164	193	197	141	145
7	280	149	170	173	157	156	184	189	134	138
8	346	198	224	227	191	190	224	229	160	165

Table 6. Average percent difference between the computed and observed runoff volumes at all hydrometric stations for the individual five years (8 datapoints), for all stations for the five years (40 datapoints), and for the total volume over the five winters (8 datapoints). The standard deviations are included for all runoff volumes and for the total station volumes.

	precipitation gauge data			radar data					
period	un-corrected gauge	gauge corrected to DFIR	gauge corrected to "bush"	raw	no scaling	mixed precip	mixed / particle shape	mixed with var. R	mixed/part with variable R
1993	-49.5	-47.8	-47.4	-19	-20.4	-10.5	-8.4	-28.2	-26.6
1994	-41.9	-33.3	-31.6	19.7	17.1	27.5	28.6	5.9	7.8
1995	-14.8	7.9	10.2	99	61.8	91.9	94.9	35.1	38.7
1996	-58	-46.7	-41	18.3	17.6	28.4	29.9	8.6	10.3
1997	-53.7	-48	-47.1	-54.1	-54.4	-46.5	-45.2	-60.9	-59.7
μ of all runoff volumes	-43.6	-33.6	-31.4	12.8	4.3	18.2	20	-7.9	-6
σ of all runoff volumes	18.4	24.7	24.9	56.6	44.9	52.9	53.4	38.2	39
μ of 5 winter total	-46.9	-37.5	-35.1	2.7	-3.7	8.8	10.5	-14.7	-12.8
σ of 5 winters	6.68	8.31	8.38	14.8	13.8	16	16.4	11.8	12.25

The volume and the peak flows of the 1995 winter hydrograph are significantly over-estimated, with the exception of the Grand River at Marsville (02GA014) and the Speed River at Armstrong Mills (02GA040) using the radar adjustment for mixed precipitation with variable R. These over-estimates are associated with the scaling of the radar. Even with the removal of scaling, some anomalous propagation was still present across the basin. Similarly, Fassnacht *et al.* (1998a) discussed this problem in terms of radar snowfall accumulation estimates and concluded that winter of 1995 provided poor radar snowfall estimates. Hollingsworth (pers. comm., 1999) stated that various lake effect events occurred in Michigan in 1995, and that the radar significantly overestimated snowfall quantities.

As the different adjustment algorithms were applied to the radar data, the simulated runoff volumes more closely approached the observed streamflows. The percent differences for the individual years and the total differences are summarized in Table 6. On average the radar provided good estimates of winter precipitation for use in hydrologic modelling. Over the five winters at the eight streamflow locations, the runoff volume from six different radar datasets was 1.53% less than observed. The differences ranged from 14.7% less total runoff volume for the mixed precipitation with variable R and particle shape radar adjustments to 10.5% more for the mixed precipitation with constant R and particle shape adjustments to the raw images. Runoff volumes and peak flows are modelled best at the mouth of the entire basin on the Grand River at Galt and for the Speed River at Armstrong Mills.

When uncorrected meteorological gauge data are used as precipitation input for hydrological modelling, the resultant modelled streamflow is approximately one-half of the observed streamflow, with the exception of 1995. Runoff volume estimates from the corrected gauge data are 17.6 and 22.2% improved over simulations with the uncorrected data, yet the DFIR and "bush" gauge precipitation yielded 37.5 and 35.1% less runoff than observed. Gauge correction did not yield more water since the three precipitation gauges operated by the University of Waterloo (UW) were situated as to resemble "bush" gauges. These UW gauges were not corrected, but only one or two were operational simultaneously. One of these gauges was operated over the entire 5 winters, while a second was only operated for the 1995 and 1996 winters and the third was only operated for part of 1997.

There may be some errors in the meteorological gauge precipitation data; but the gridding of the gauge data using the inverse square distance method smears storm events that approach the study watershed. This is important since the two gauges located within the basin are not operated continuously; one gauge was operated only for part of one winter season and the other gauge is maintained only during business hours (8:00 EST to 17:00 EST). Precipitation events tend to approach the watershed from the west (lake effect storms) or the south-west (jet stream storms), and the gridding of the gauge precipitation data does not observe actual storm movement while radar data tends to preserve the shape of storm events. While there are problems inherent with the gridding technique used to develop the areal precipitation estimates using a limited number of precipitation gauges, it is doubtful that an alternate gridding technique or the inclusion of more station data will improve the runoff volumes by the deficit 35%. Use of precipitation estimates from additional gauges should nevertheless improve the shape of the storm events and provided gridded precipitation data more closely resembling the pattern illustrated in radar images. A combination of the corrected gauge and the radar data, such as the rainfall scheme devised by Brandes (1975), may help alleviate some of the problems from either precipitation data source.

The removal of scaling improves the flow estimates compared to the use of raw radar. The adjustments for mixed precipitation using a constant R and the addition of the particle shape adjustment factor typically do not further degrade the flow estimate and in some cases improve the estimates. As a continuation of Fassnacht *et al.* (1998a), ongoing research has illustrated that the use of variable R for the adjustment of mixed precipitation does not improve the snowfall accumulation estimates over the use of constant R; the modelled streamflow volumes are underestimated by using the variable R. To refine the adjustments, a site specific probability of snow curve should be derived as a function of air temperature and the local lapse rate between particle formation height and surface air temperature should be examined. Similarly the applicability of the particle shape adjustment factor and the variability of the surface area to mass ratio as a function of crystal formation temperature should be investigated.

Simulating runoff volumes can be adequately accomplished by using various forms of adjusted radar, however, as mentioned above, peak flows are not simulated as accurately. While the vertical water and energy modelling by CLASS represents most of the physical processes associated with snow and winter hydrology, additional modellling developments will further improve the streamflow simulation, specifically this can improve the timing and quantity of the peak flow.

CONCLUSIONS

Weather radar provided better estimates of winter precipitation for hydrologic modelling than uncorrected and corrected gridded gauge data, in terms of runoff generation. The first improvement to the radar data was the removal of any image scaling greater than the lowest possible increment. Further improvements in the modelled streamflow were made by adjusting the radar snowfall estimates using algorithms that are a function of air temperature; including the precipitation rate in the

adjustment of mixed precipitation yielded streamflow underestimates, whereas using a constant rainfall adjustment factor yielded streamflow overestimates. The use of a particle snowflake shape adjustment factor for temperature below freezing slightly enhanced the improvements made by the mixed precipitation adjustments for melting temperatures.

While the peak flows were simulated adequately using weather radar precipitation input, the runoff volumes more closely matched observed volumes. Improvements to the peak flow estimation are expected with the incorporation of advanced snow processes into the model. To further investigate the precipitation gauge data, more data are required and the data gridding should be revisited. To refine the radar adjustments, the following should be investigated: removal of the scaling problems, a site specific probability of snow curve as a function of air temperature, the local lapse rate, the pattern of the particle shape curve, and the relationship between the surface area to mass ratio and the crystal formation temperature.

ACKNOWLEDGMENT

This research was supported by Atmospheric Environment Service science subventions and by AES-CRYSYS funding. The radar images were provided by AES King City Radar, and meteorologic data were provided by AES-Downsview. The assistance of the personnel providing these data is acknowledged with thanks. Thanks are also due to Dr. H. Goertz of Water Survey of Canada for supplying an advanced copy of the 1997 HYDAT data. A discussion at the 56th ESC in Fredericton with Jane Hollingsworth of the National Weather Service Indiana Office provided information into the radar problems of snowfall estimation during the 1995 and 1997 winters. Comments by Barry Goodison, Shari Carlaw, Jayson Innes, Frank Seglenieks, and three anonymous reviewers helped strengthen this paper and improve its readability.

REFERENCES

Auer, A.H., Jr. (1974) The rain versus snow threshold temperatures. *Weatherwise*, **27**:67.

Brandes, E.A. (1975) Optimizing rainfall estimates with the aid of radar. *Journal of Applied Meteorology*, **14**(10): 1339-1345.

Bussieres, N. and W. Hogg (1989) The objective analysis of daily rainfall by distance weighting schemes on a mesoscale grid. *Atmosphere-Ocean*, **27**(3):521-541.

Cole, J.A., C. Wade and R.M. Rasmussen (1998) Evaluation of precipitation gauges and wind shielding for the measurement of real-time liquid-equivalent snowfall. *Presentation at the 55th Eastern Snow Conference*, Jackson, New Hampshire, June 3-5, 1998.

Crozier, C.L., P.I. Joe, J.W. Scott, H.N. Herscotvitch and T.R. Nichols (1991) The King City operational Doppler radar: development, all season applications and forecasting. *Atmosphere-Ocean*, **29**:479-516.

Environment Canada (1997) *1996 HYDAT Hydrometric Data CD-ROM.* Water Survey of Canada, Ottawa, Canada.

Environment Canada (1998) CMC Climate And Water Information: Canadian Climate Station Catalogue. URL: <http://www1.tor.ec.gc.ca/csc/query.asp>, Climate And Water Information, Canadian Meteorological Centre, Atmospheric Environment Service, Downsview, Ontario, Canada.

Fassnacht, S.R., E.D. Soulis, K.R. Snelgrove and N. Kouwen (1998a) Application of weather radar to model the snow hydrology of southern Ontario. In *Proceedings of the 55th Annual Eastern Snow Conference*, Jackson, New Hampshire, p115-123.

Fassnacht, S.R., E.D. Soulis, K.R. Snelgrove and N. Kouwen (1998b) Hydrologic modelling of the

snowpack in southern Ontario. *Presentation at the 55th Annual Eastern Snow Conference*, Jackson, New Hampshire, June 3-5, 1998.

Finnerty B.D., M.B. Smith, D.J. Seo, V. Koren and G.E. Moglen (1997) Space-time scale sensitivity of the Sacramento model to radar-gage precipitation inputs. *Journal of Hydrology*, **203**:21-38.

Fujiyoshi, Y., T. Endoh, T. Yamada, K. Tsuboki, Y. Tachibana and G. Wakahama (1990) Determination of a Z-R relationship for snowfall using a radar and high sensitivity snow gauges. *Journal of Applied Meteorology*, **29**(2): 147-152.

Goodison, B.E. (1978) Accuracy of canadian snow gauge measurements. *Journal of Applied Meteorology*, **17**: 1542-1548.

Goodison, B.E. and J.R. Metcalfe (1992) The WMO Solid Precipitation Intercomparison: Canadian Assessment. In *WMO Technical Conference on Instruments and Methods of Observation*, WMO/TD No. 462, 221-225.

Goodison, B.E., P.Y.T. Louie and D. Yang (1998) *WMO Solid Precipitation Measurement Intercomparison Final Report*. WMO Instruments and Observing Methods Report No. 67, WMO/TD No. 872.

Houck, R.E., J. Waldstreicher, J.M. Hassett and P.F. Blottman (1995) Preliminary investigation of WSD-88D data for winter hydrometeorological events in upstate New York. In *Proceedings of the 52nd Annual Eastern Snow Conference*, Toronto, Ontario, p39-50.

Kouwen, N. and G. Garland (1989) Resolution considerations in using radar rainfall data for flood forecasting. *Canadian Journal of Civil Engineering*, **16**:279-289.

Kouwen, N., E.D. Soulis, A. Pietroniro, J.R. Donald and R.A. Harrington (1993) Grouped response units for distributed hydrologic modelling. *ASCE Journal of Water Resources Planning and Management*, **119**(3):289-305.

Lautensach, H. and R. Bogel (1956) Der Jahrsgang des mittleren geographischem Hohengradienten der Lufttemperatur in den verschiedenen Klimagebieten der Erde. *Erdkunde*, **10**, 270-282.

Marsh, P. (1990) Snow Hydrology. In *Northern Hydrology: Canadian Perspectives* (eds. T.D. Prowse and C.S.L. Ommanney), National Hydrology Research Institute, Saskatoon, Canada.

Marshall J.S. and W.M. Palmer (1948) The distribution of raindrops with size. *Journal of Meteorology*, **5**:165-166.

Matrosov, S.Y. (1998) A dual-wavelength radar method to measure snowfall rate. *Journal of Applied Meteorology*, **5**: 165-166.

Matsuo, T., Y. Sasyo and Y. Sato (1981) Relationship between types of precipitation on the ground and surface meteorological elements. *Journal of the Meteorological Society of Japan*, **59**, 462-476.

Mould, B. (1985) Powerline. In *New Day Rising*, SST Records, Lawndale, CA.

Ohtake, T. and T. Henmi (1970) Radar reflectivity of aggregated snowflakes. Preprints of the *14th Radar Meteorology Conference*, American Society of Meteorology, p209-210.

Richards, W.G. and C.L. Crozier (1983) Precipitation measurement with a C-band weather radar in southern Ontario. *Atmosphere-Ocean*, **21**: 125-137.

Ryzhkov, A.V. and D.S. Zrnic (1998) Discrimination between rain and snow with a polarimetric radar. *Journal of Applied Meteorology*, **37**(10): 1228-1240.

Seglenieks, F.R., E.D. Soulis, K.R. Snelgrove, N. Kouwen, S.R. Fassnacht, A.K.Graham, M. Lee, and S.I. Solomon (1997) Integrated hydrologic modelling for MAGS. *Presentation at the 3rd Mackenzie GEWEX Study Workshop*, Atmospheric Environment Service, Downsview, Ontario, November 17-19, 1997.

Sekhon, R.S. and R.C. Srivastava (1970) Snow-size spectra and radar reflectance. *Journal of Atmospheric Sciences*, **27**:299-307.

Soulis, E.D., K.R. Snelgrove, N. Kouwen and D.L. Verseghy (1999) Toward closing the vertical water balance in Canadian atmospheric models: Coupling of the land surface scheme CLASS with the distributed hydrological model WATFLOOD. Accepted to the *Atmosphere-Ocean*, September 1998.

Tabios, G.Q., III and J.D. Salas (1985) A comparative analysis of techniques for spatial interpolation of precipitation. *Water Resources Bulletin* , **21**(3): 365-380.

Tao, T., and N. Kouwen (1990) Remote sensing and fully distributed modelling for flood forecasting. *Journal of Water Resources Planning and Management* , **115**(6): 809-823.

Thiessen, A.H. (1911) Precipitation averages for large areas. *Monthly Weather Review*, **39**(7):1082-1084.

Verseghy, D.L. (1991) CLASS-A Canadian Land Surface Scheme for GCMs. I. Soil model. *International Journal of Climatology* , **11**:111-133.